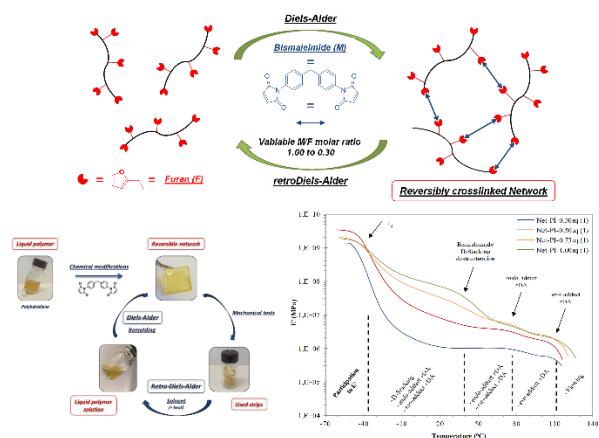


Reprocessable covalent elastomeric networks from functionalized 1,4-*cis* polyisoprene and polybutadiene

Pierre Berto †, Jérémy Mehats †, Anne-Laure Wirotius †, Stéphane Grelier † and Frédéric Peruch *†

† Univ. Bordeaux, CNRS, Bordeaux INP/ENSCBP, Laboratoire de Chimie des Polymères Organiques, UMR 5629, 16 avenue Pey-Berland, F-33607 Pessac Cedex, France

For Table of Content Use Only



ABSTRACT

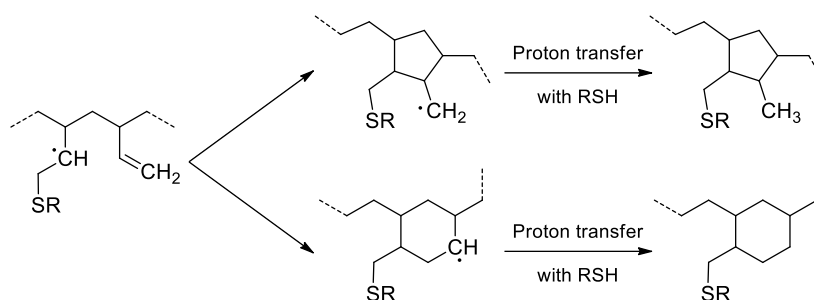
To obtain and maintain rubber properties such as elasticity, strength, creep and chemical resistance, or stiffness over time, rubbers must be chemically cross-linked, mainly, by sulfur vulcanization. However, the materials produced in this manner result in irreversibly cross-linked

networks and are consequently difficult to recycle, which leads to large quantities of rubber waste each year. In this paper, a new route to synthesize reversibly cross-linked 1,4-*cis* PI and PB based on the Diels-Alder chemistry is investigated. Furan groups are firstly grafted along the polymeric backbone and at chain-ends. In a second step, a bis-maleimide compound is added to the modified liquid material, leading to the formation of a thermo-reversible cross-linked elastomers. Mechanical properties of the resulting rubber can be easily tuned and depend on the bis-maleimide / furan ratio as well as on the nature of the polymeric precursor (polyisoprene vs polybutadiene). The good reprocessability of these materials was demonstrated by remolding them 5 times without any loss of properties between the first and the last cycle.

INTRODUCTION

Thermosets are currently used in a large range of applications going from building materials to aerospace equipment. Due to the cross-linking method currently used, these materials cannot be reshaped or easily recycled at the end of their use. On the contrary, thermoplastics can flow above a certain temperature allowing an easier processability and the recyclability of the material.¹ Elastomers, like polyisoprene (PI) and polybutadiene (PB) used in tire industry, belong to the thermoset materials. In order to improve the mechanical properties, solvent and gas permeability, creep resistance and elasticity, the polymeric chains have to be cross-linked, mainly through a vulcanization process (sulfur cross-linking method discovered by Charles Goodyear in 1839).^{2,3} As a consequence, recyclability of such materials is complicated and a huge quantity of rubber waste is generated each year. To overcome this constraint, scientists put many efforts to develop reversible crosslinking of the polymeric chains. Generally, reversible crosslinking could be classified into two categories: the noncovalent interactions (hydrogen bonding, ionic interaction or metal coordination) and the dynamic covalent bonds.⁴⁻¹⁰ Elastomeric materials based on weak

noncovalent interactions generally exhibit reduced mechanical properties or a poor solvent resistance compared to the chemically crosslinked materials. On the other hand, elastomers based on dynamic covalent bonds like imine bonds, transesterification reactions, disulfide exchange, alkoxyamine or Diels-Alder reactions present generally higher moduli, strength, elasticity, chemical and stress cracking resistance.^{11–13,7,14} Properties of the PI and PB rubbers are highly dependent on the microstructure of the repeating units (1,4-*trans*, 1,4-*cis*, 1,2 and 3,4-units for PI).¹⁵ Indeed, the 1,4-*cis* microstructure is often sought due to its enhanced mechanical properties such as lower T_g or crystallization phenomenon occurring under stress.¹⁶ Several reversible cross-linked polymers networks based on the Diels-Alder reaction have already been described.^{17–23} Generally, furan groups are grafted through the thiol-ene reaction onto the 1,2- vinylic (15 %) units of a high molar mass PB ($M_w = 460\,000\text{ g}\cdot\text{mol}^{-1}$).³ After addition of a bis-maleimide, the storage modulus was increased by one order of magnitude due to the cross-linking. Other studies have also described the synthesis of reversible PB networks by grafting furan groups or carboxylic acids and amines through thiol-ene reactions, using the 1,2-vinylic units.^{24,25} However, in all cases, the starting polymer had a high molar mass ($> 150\,000\text{ g}\cdot\text{mol}^{-1}$) and a high content of 1,2-units (15 to 90 %). Besides, the viscosity being linked to the polymer chain length, an increase of the latter renders handling and processability of these materials more complex. In addition, well-known thiol-ene side reactions can occur during the synthesis processes like chains coupling or 1,2-units cyclization (Scheme 1).^{22,26–32} Improvement of the mechanical properties of the networks cannot therefore be attributed only to the formation of the reversible network, but also to the side reactions. We have already demonstrated that reprocessable PB or PI network can be obtained by modification of the polymeric end-chain groups. Properties of the reversible cross-linked elastomers can be easily tuned by modulation of the chain lengths or the cross-linking density.^{33,34}



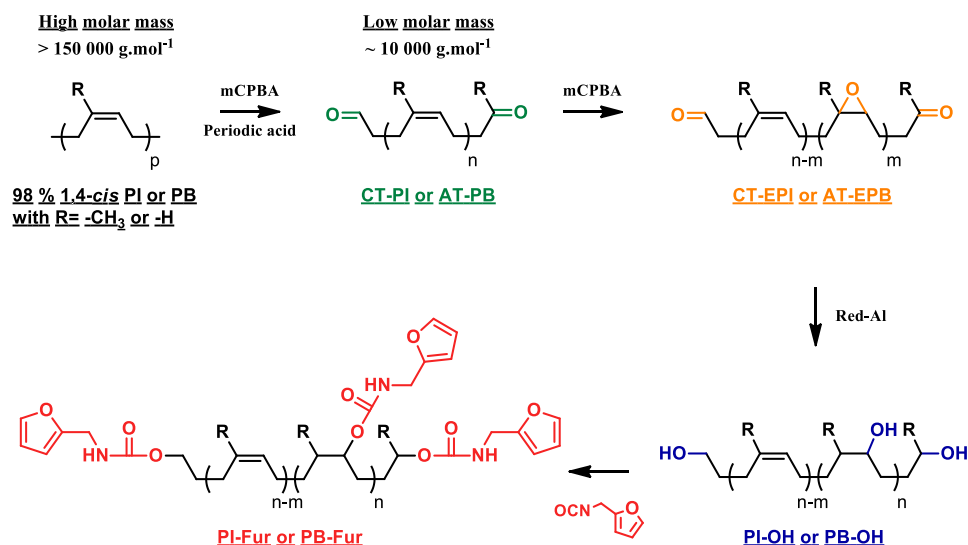
*Scheme 1: Cyclisation side-reaction during thiol-ene addition on 1,2 units of polybutadiene.*²⁶

In this study, reversible and well-defined rubber networks were synthesized from liquid low molar mass ($\sim 10\,000\text{ g}\cdot\text{mol}^{-1}$) PB or PI with a high 1,4-*cis*-units (98 %) content, obtained from the controlled degradation of high molar mass 1,4-*cis*-PI and 1,4-*cis*-PB.³⁵ The use of a low molar mass polymer allows better chemical characterization, shorter solubilization time, easier purification, better processability and molding of the final material. After two chemical modifications steps, furan groups were grafted both along the backbone and at the chain-ends of the polymers. Finally, addition of a bis-maleimide (BM) to the liquid furan modified PI of PB (PI-Fur of PB-Fur) led to the formation of a thermo-reversible network. After an accurate chemical characterization of the polymer intermediates, the impact of the bis-maleimide / furan molar ratio on the mechanical properties of the material was investigated. In the final step, the reprocessability of the reversible elastomeric network was assessed.

RESULTS AND DISCUSSIONS

Polymer synthesis and characterization

Low molar mass polyisoprene (PI) and polybutadiene (PB) with a high 1,4-*cis*-units content (over 98 %) containing furan group along the backbone and at both chain-ends (PI-Fur and PB-Fur) were synthesized starting from a high molar mass 1,4-*cis* PI and PB (Scheme 2).



Scheme 2: General synthetic route for the synthesis of 1,4-cis low molar mass PI-Fur and PB-Fur.

A carbonyl telechelic polyisoprene (CT-PI) and an aldehyde telechelic polybutadiene (AT-PB) with a molar mass of $10\,000\text{ g}\cdot\text{mol}^{-1}$ were first prepared by a controlled degradation of the PI and PB (epoxidation with mCPBA followed by the oxirane rings cleavage with periodic acid).^{35–37} Then, around 10 % of the repeating units of CT-PI and AT-PB were epoxidized with mCPBA to yield to a carbonyl telechelic epoxidized polyisoprene (CT-EPI) and a aldehyde telechelic epoxidized polybutadiene (AT-EPB). The epoxy units and terminal carbonyl groups were finally simultaneously reduced by sodium bis-(2-methoxyethoxy) aluminate hydride (Red-Al) to obtain the polyisoprene and polybutadiene containing hydroxyl groups at both chain-ends and along the backbone (PI-OH and PB-OH, Scheme 2).³⁸ Finally, furfuryl-isocyanate was reacted with the hydroxyl group to lead to the formation of a PI and a PB containing furan group along the backbone and at both chain-ends (PI-Fur and PB-Fur). During the synthesis process, all intermediates have been characterized by Size Exclusion Chromatography (SEC) and ^1H Nuclear Magnetic Resonance (^1H NMR) analyses to confirm the absence of side reactions. For instance, SEC

chromatograms of the different intermediates are perfectly superimposed (Figure S1) showing the absence of uncontrolled cross-linking that could have occurred during the modification steps. ^1H NMR spectra of the PB intermediates are represented on Figure 1. The signal at 9.77 ppm (peak 1, Figure 1a) corresponding to the aldehyde protons of the AT-PB chain-ends allows to evaluate the degree of polymerization of the polymer chain after degradation ($\text{DP} = 187$). Epoxidation of AT-PB lead to the formation of the AT-EPB, a new signal corresponding to the epoxy units appeared at 2.92 ppm, allowing to calculate the amount of epoxy units (peak 6, Figure 1b). Here, 11 % of the butadiene units were epoxydized, meaning that each polymeric chain contains a mean of 20-21 epoxy units (calculations detailed in ESI).

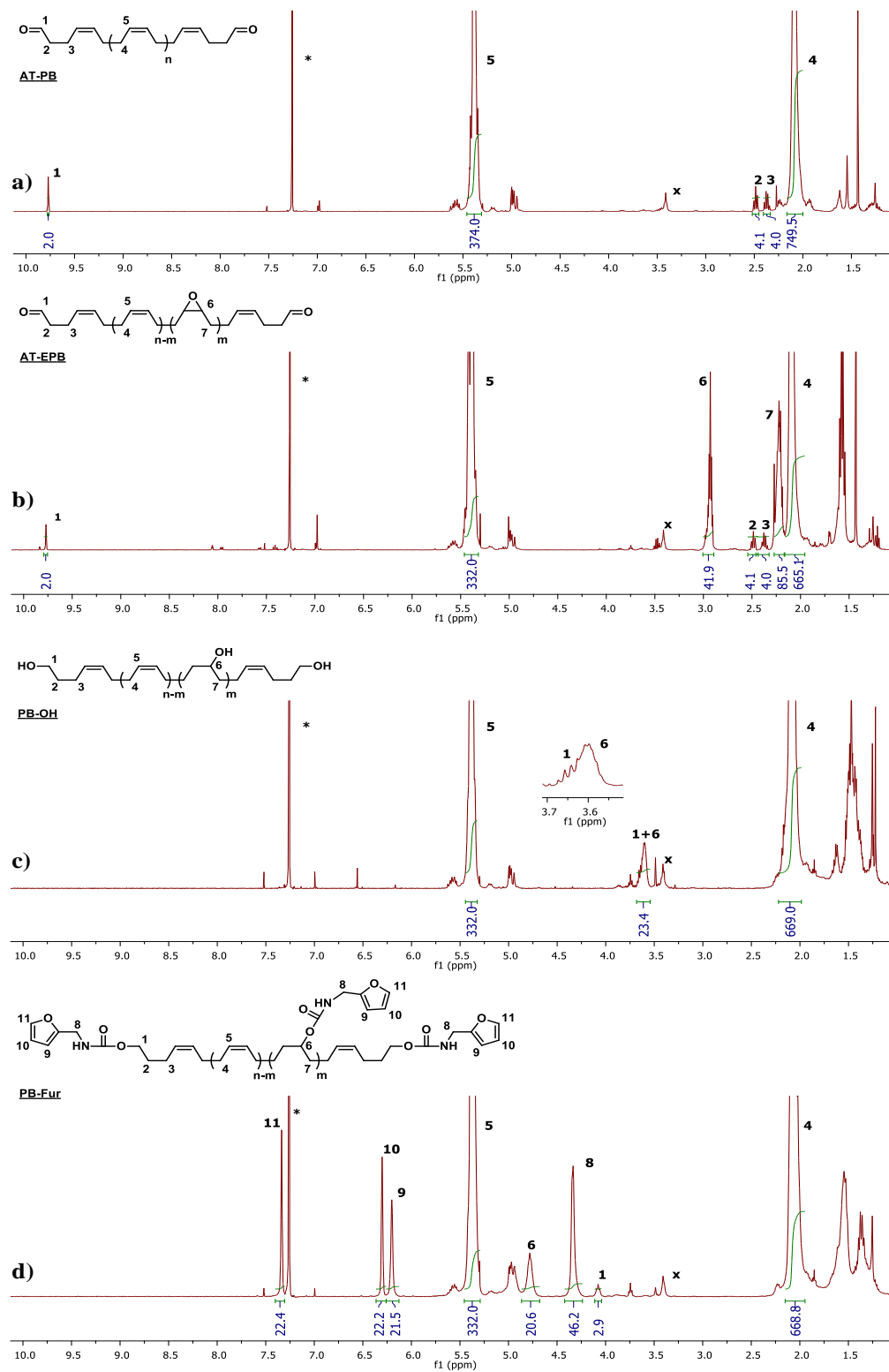


Figure 1: ^1H NMR characterization of the PB intermediates during the synthesis (x: signal present in the initial polymer, *: CDCl_3)

After reduction of the oxirane rings by the Red-Al, PB-OH is obtained. The signals at 2.92 ppm and at 9.77 ppm completely disappeared and two new signals appeared around 3.55-3.70 ppm (peak 1+6, Figure 1c). The multiplet at 3.60 ppm corresponds to the protons linked to carbons bearing hydroxyl groups (-CH(OH)-) along the PB chain, and the second one (triplet at 3.65 ppm) is associated to protons linked to the carbons of the hydroxyl chain-end (-CH₂-OH). The complete disappearance of the epoxy units confirmed the completion of the reaction. Finally, after reaction with furfuryl isocyanate, it was possible to assume a full conversion of all the hydroxyl groups thanks to the presence of new peaks (peaks 9, 10 and 11 at 6.20, 6.30 and 7.34 ppm respectively, Figure 1d) corresponding to the furanic protons. Moreover, shift of the peak 1 from 3.65 ppm to 4.10 ppm also confirmed the reaction of the hydroxyl groups presents at the chain ends. ¹H NMR characterization of the PI series intermediates are presented in supporting information section (Figure S2). Similar observations concerning the appearance, disappearance and shift of peaks can be done confirming the obtention of a furan modified polyisoprene (PI-Fur).

The backbone modification was also confirmed by Differential Scanning Calorimetry (DSC) analyses. A gradual *T_g* shift is observed after each step of the backbone modification. For PI, the *T_g* shifted from -64 °C for CT-PI to -48 °C for PI-Fur. Similarly, *T_g* went from -104 °C for AT-PB to -84 °C for PB-Fur (Figure S3 and Table S1). Besides, whereas AT-PB was able to crystallize at -40 °C (a well-known phenomenon already observed³⁴), after modification of the backbone, crystallization was no more observed.

Properties of the elastomers

As shown on Figure 2, the liquid PI-Fur or PB-Fur are mixed with the bis-maleimide to obtain a thermo-reversible network based on the Diels-Alder reaction. To tune the properties of these

elastomeric materials, the amount of bis-maleimide was varied with a maleimide/furan molar ratio ($R_{M/F}$) going from 1.00 to 0.30 eq. The resulting properties were compared.

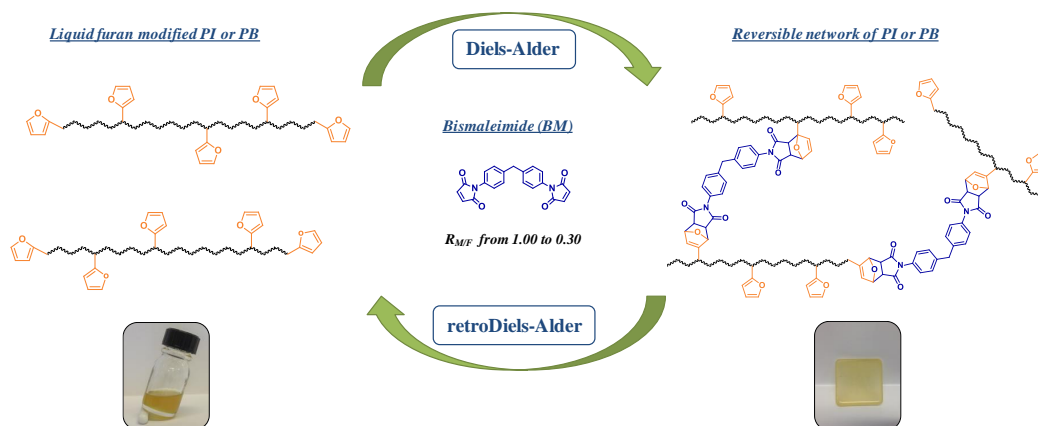


Figure 2: Schematic representation of the formation and reprocessability of the reversible cross-linked PI and PB network based on the Diels-Alder chemistry.

To evaluate the efficiency of the cross-linking, swelling tests were first performed to evaluate the soluble fraction of the obtained elastomer. In each case and whatever the $R_{M/F}$ used, the soluble fraction was always low (less than 6 %) even for the lowest cross-linked material ($R_{M/F} = 0.30$, Figure 3 and Table S2). For the PI based networks, the soluble fraction is equal to 5.6 % for the lowest crosslinked material ($R_{M/F} = 0.30$) and decrease to 0.3 % when $R_{M/F} = 1.00$. A similar tendency is observed for the PB based elastomers. The swelling degree confirms the efficiency of the cross-linking reaction. For example, swelling rate of the PI based networks decreased from 850 % to 400 % when the $R_{M/F}$ increases from 0.30 to 1.00. This behavior was expected, as a lower $R_{M/F}$ would lead to a lower cross-linking density, allowing a higher swelling of the network. Similar trend is observed for the PB based elastomers; the swelling rate of the material decreased from 570 % to 280 % for $R_{M/F}$ going from 0.30 to 1.00.

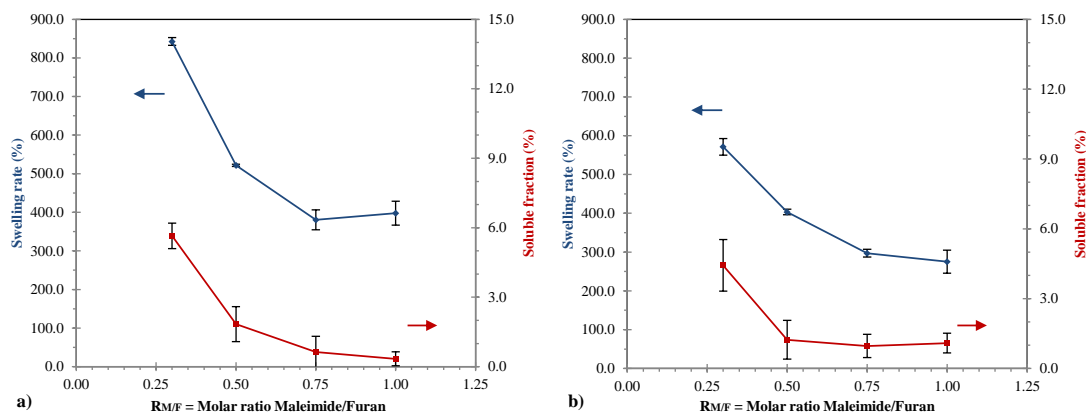


Figure 3: Swelling test of the PI (A) and PB (B) networks as a function of $R_{M/F}$.

Mechanical properties of the prepared networks were characterized by tensile test and DMA (Figure 4 and Table S3). Tensile test analyses revealed that the Young's modulus (E) of the elastomers is highly impacted by $R_{M/F}$. E is equal to 1 MPa for $R_{M/F} = 0.30$ and rises to 60 MPa for the highest $R_{M/F}$ for the PI elastomers. For the PB based networks E reaches a value of 240 MPa when $R_{M/F} = 1.00$. A similar behavior was observed for the stress at break, which increased with $R_{M/F}$, from 1 MPa for $R_{M/F} = 0.30$ up to 10 and 16 MPa for $R_{M/F} = 1.00$ for PI and PB networks respectively. This could be easily explained as an increase of $R_{M/F}$ would increase the cross-linking density and thus the strength of the network. Therefore, whatever the $R_{M/F}$, PB networks exhibited higher values of Young's modulus and stress at break than PI networks. This difference can be attributed to the cross-linking density differences obtained in the two types of networks. Indeed, even if the molar mass of the precursors is roughly the same, the DP is different as the molar mass of the repeating units is different (68 g/mol for isoprene and 54 g/mol for butadiene). Consequently, for a same percentage of modification, the number of functional groups per chains is higher for PB than for PI, increasing then the cross-linking density and thus the modulus.

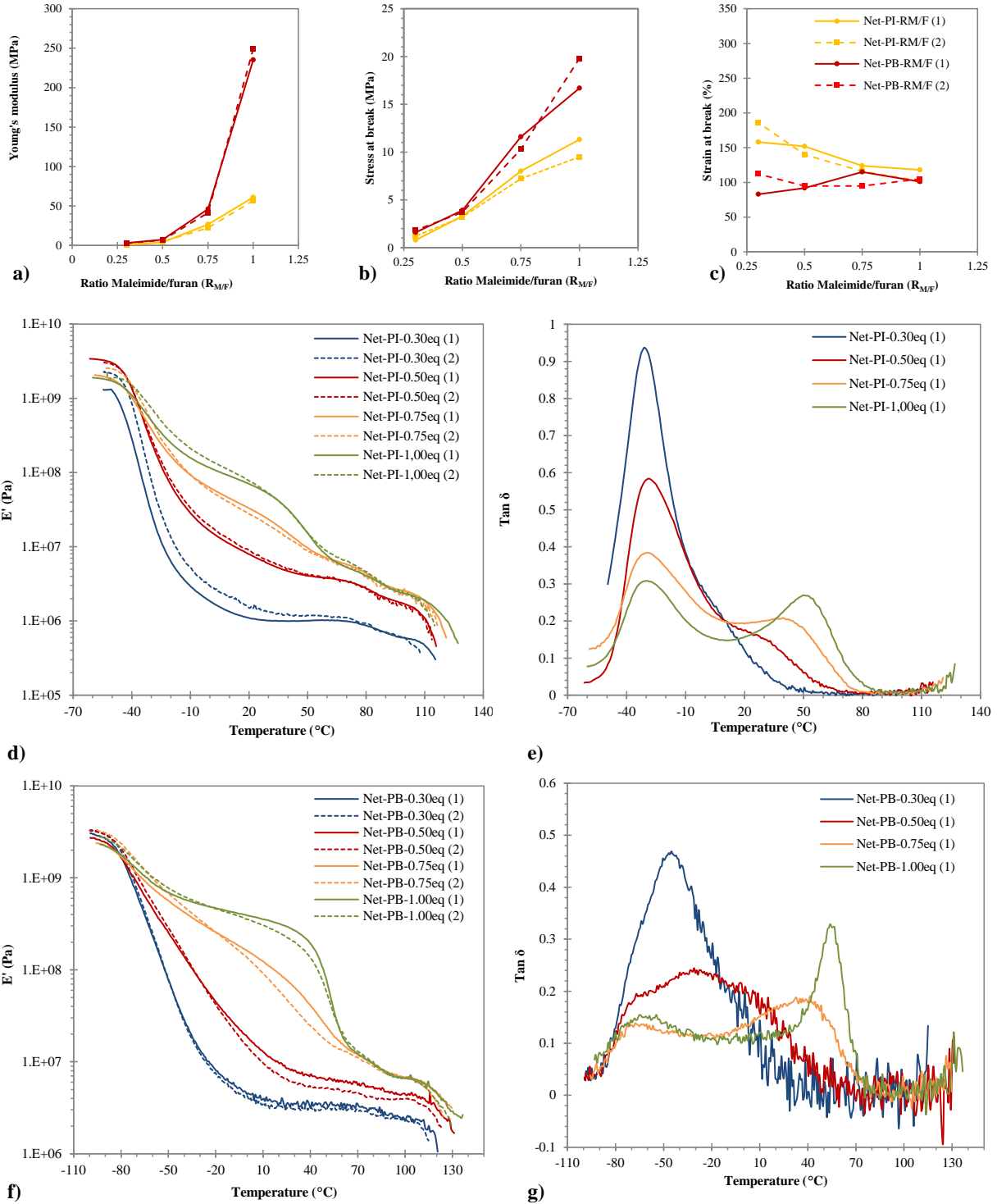


Figure 4: Tensile test analyses of the PI and PB networks a) Young modulus vs $R_{M/F}$ b) Stress at break vs $R_{M/F}$ c) Strain at break vs $R_{M/F}$. DMA analyses of the network of PI as a function of $R_{M/F}$. d) storage modulus E' e) $\tan \delta$ and of the network of PB as a function of $R_{M/F}$. f) storage modulus E' g) $\tan \delta$. Dotted lines of all traces represents the result analyses of the corresponding reprocessed material (1) = first molding, (2) = reprocessed.

On the contrary, the strain at break was less affected by $R_{M/F}$. Elongation at break for the PI based materials went from 170 % for $R_{M/F} = 0.30$ to 110 % for $R_{M/F} = 1.00$. For the PB based networks, the strain at break oscillated between 90 % and 110 % whatever the quantity of bis-maleimide (Figure 4c).

Compared to a previous study where only the polymer chain-ends were functionalized to cross-link the polymers, the Young's modulus, the stress at break and strain at break for 10 000 $\text{g}\cdot\text{mol}^{-1}$ PB based networks was equal to 3.5 MPa, 2.9 MPa and 160% respectively.³⁴ Increasing the amount of cross-linking points by adding furfuryl groups along the backbone lead to a material with improved mechanical properties.

Reprocessability ability of the networks were then investigated. To this end, used strips coming from previous mechanical analyses were remolded after being heated in chloroform at 120 °C in a closed vessel to induce the retro Diels-Alder reaction. Reprocessed strips were then analyzed, and results are shown on Figure 4a-c (dotted lines) and in Table S3. In all of cases, the reprocessed material exhibited the same properties as the first ones obtained from the first molding. Values of the Young's modulus, strain or elongation at break are the same, showing the excellent reprocessability properties of these elastomers.

To go further, DMA analyses were performed, and traces obtained for the PI networks are represented on Figure 4d and e. As expected, the $R_{M/F}$ has no impact on the T_g of the material, it is equal to $\sim -40/-30$ °C (peak of the $\text{Tan } \delta$) for each elastomer. On the contrary, the storage modulus (E') was dramatically affected by the quantity of bis-maleimide. For the $R_{M/F}$ of 0.30, two rubbery plateaus can be observed: a first one between -10 °C and 75 °C with a value of E' close to 1 MPa and a second one between 80 and 105 °C with an storage modulus of 0.6 MPa (Figure 4d, blue line). Over 110-120 °C and due to the rDA reaction, the material lost its properties and started to

flow. The first drop of modulus observed at 80 °C could be explained by the occurrence of the *rDA* reaction of the *endo*-adducts. Indeed, two adducts (*endo* and *exo*) are formed after the DA reaction between a furan and maleimide group. The *endo* adduct (kinetic adduct) is less stable than the *exo* one and exhibits a lower *rDA* temperature.³⁹ When $R_{M/F}$ was increased to 0.50 (Figure 4d, red line), the two rubbery plateaus at 3.4 and 2.0 MPa for the first and second plateau respectively can still be observed. Again, the drop at 80°C is attributed to the *rDA* of the *endo*-adduct. In addition, the observed modulus increase can be explained by the higher cross-linking density as observed for the tensile tests analyses. For the elastomer with $R_{M/F}$ of 0.75 and 1.00, a general increase of the modulus plateau values was observed. More surprisingly, a third modulus drop was observed at 50°C (Figure 4d, orange and green traces). This transition is confirmed by the peak observed at 50 °C on the loss modulus ($\text{Tan } \delta$, Figure 4e orange and green traces) for both elastomers. The first peak at -40 °C, corresponding to the T_g , decreased with $R_{M/F}$ whereas the second transition observed at 50 °C increased with $R_{M/F}$. This second transition could be associated to the π -stacking induced by the BM compound contained in the formulation and/or the hydrogen bonds formed via the urethane functions created during the grafting of the furfuryl units. For low $R_{M/F}$, the quantity of BM in the network was probably too low to allow these non-covalent interactions, whereas for higher $R_{M/F}$, the relative quantity of BM compared to the PI increase and enables the π -stacking.

Concerning the PB based networks, DMA characterization results are shown on Figure 4f and g and all the modulus values are reported in Table S3. Linked to the structural differences between PB and PI, PB based elastomers exposed a lower T_g (-80°C), whatever the $R_{M/F}$ used. Again, when the $R_{M/F}$ is equal to 0.30 or 0.50, two rubbery plateaus are observed: a first between T_g and 80°C and a second one between 80°C to 130°C. The transition at 80°C is associated to the *rDA* of the

endo-adduct whereas the transition at 130°C corresponds to the flowing of the material, linked to the *rDA* of the *exo*-adduct. For the $R_{M/F}$ of 0.75 and 1.00 a third plateau appears once again between T_g and 50 °C. Here, the impact of the π -stacking and/or the H-bonding through urethane functions is more pronounced than for PI based elastomers and values of the modulus in the rubbery plateau reach 320 MPa between T_g and 50°C for PB based elastomers with the higher $R_{M/F}$. The transitions at 50°C can clearly be observed on the loss modulus of PB based elastomers with the higher $R_{M/F}$ (Figure 4g). Besides, the values of the storage modulus plateau were always superior for the PB networks than the PI ones. Finally, DMA analyses of the reprocessed networks was performed like for tensile test analyses. Traces obtained are represented in dotted lines on Figure 4d and f. Again, an excellent superimposition of the DMA traces for both PI and PB based elastomers was observed, confirming the good reprocessability ability of these materials.

Finally, the elastomers were analyzed by DSC, thermograms are represented on Figure 5 and values are given in Table S4. As observed in DMA, T_g of the elastomer is independent of the $R_{M/F}$ used and is respectively equal to - 46 °C and - 83 °C for PI and PB based networks respectively. At higher temperature, two endothermic peaks are observed between 75 °C and 160 °C, the one at the lowest temperature corresponds to the *endo*-adducts of the *rDA* reaction whereas the other corresponds to the *exo*-adducts.^{25,26} The temperature values of the *rDA* reactions measured by DSC are in good agreement with the results observed in DMA where the material flowing was observed around 120-130 °C. Besides, enthalpy value of the *rDA* peaks increased with $R_{M/F}$: from 9.1 J/g for $R_{M/F} = 0.30$ to 23.8 J/g for $R_{M/F}=1.00$ for PI networks. Concerning PB based network, the increase of enthalpy is higher: from 13.3 J/g for $R_{M/F} = 0.30$ to 42.2 J/g for $R_{M/F}=1.00$. This behavior is in accordance with the increase of the number of DA adducts with the $R_{M/F}$. Besides, an endothermic transition appears between 10 and 70 °C, where the values of the enthalpy peak

increase with the $R_{M/F}$ (Figure 5c, d and Table S4). This could be linked to the one previously observed in DMA, confirming the π -stacking and/or H-bonding or urethane functions impact on the properties of the material. These aggregation phenomena were further confirmed by the shape of the tensile test curves, where for the higher $R_{M/F}$, a strong increase of the stress is observed for strains below 20 % followed by a linear increase of the stress vs the strain (Figure S4). This hypothesis agrees with the second transition observed in DMA at 50°C (Tan δ - Figure 4e and g): as the tensile tests were performed at 22°C.

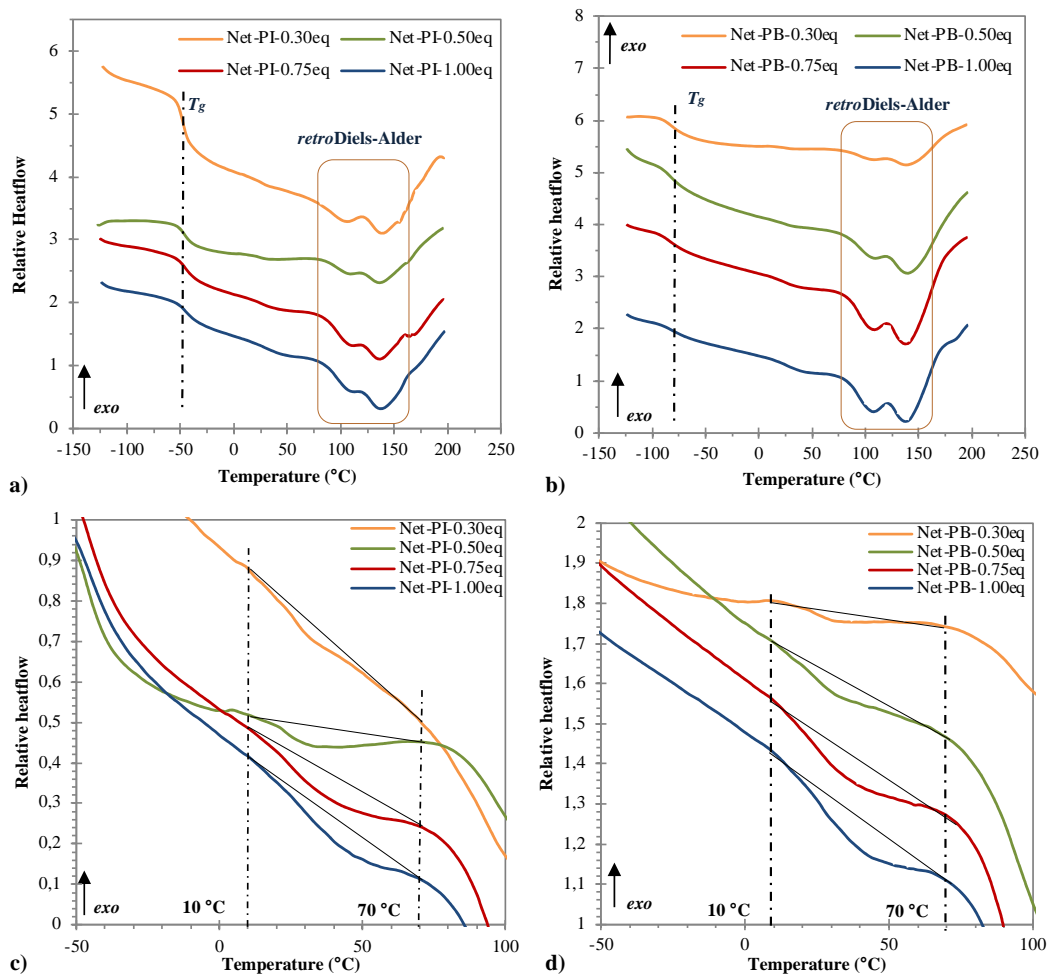


Figure 5: DSC thermograms a) PI networks b) PB networks c) zoom between 10 and 70 °C, for PI networks d) zoom between 10 and 70 °C, for PB networks.

Reprocessability of the elastomers

Reprocessability ability of the materials synthesized in this study was investigated over 5 cycles of reprocessing on PI network with $R_{M/F} = 0.50$. Tensile test analyses revealed an excellent stability of the reprocessed elastomer properties even after 5 cycles of reprocessing (Figure 6 and Table S5). For instance, the Young's modulus was measured between 4 and 5 MPa and the stress at break around 3.5 MPa, whatever the reprocessing cycle. The measured strain at break was also constant over reprocessing cycle and was around 160 % even after 5 cycles. DMA analyses confirmed the previous observations: traces of the storage modulus (E') is nearly overlapped for all reprocessing cycle (Figure 6).

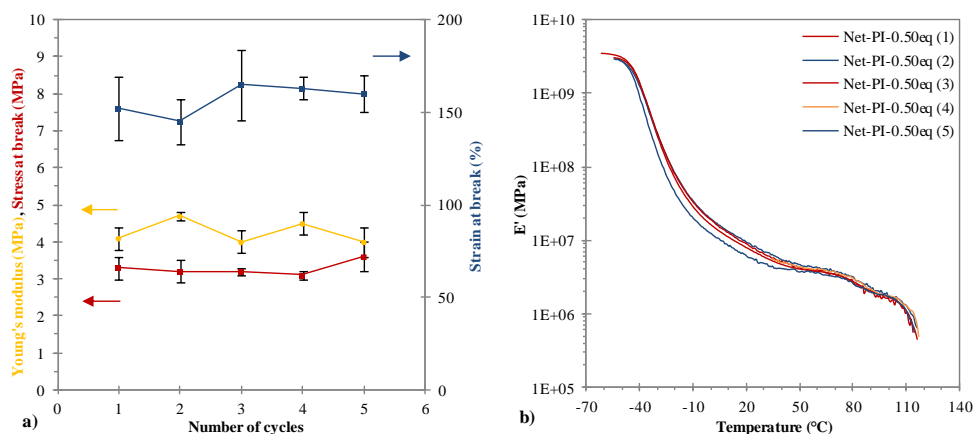


Figure 6: Tensile tests and DMA analyses of Net-PI-0.50 eq over 5 reprocessing cycles (a) Young's modulus, stress at break and strain at break obtained by tensile analyses. (b) Storage modulus (E') traces obtained by DMA.

Values of T_g , modulus and flowing temperature were also very close for all cycles (Table S5). All these results clearly show the excellent reprocessing ability of these polymers. Indeed, even after mechanical tests where the material is heated and stressed (tensile tests and DMA), the reprocessed material has identical properties even after 5 cycles of reprocessing.

Conclusions

In this study, reversible covalent polymer networks with high reprocessing ability were prepared through a well-defined and controlled chemistry (no side reaction or uncontrolled cross-linking occurred during the synthesis or the reprocessing). To this end, 1,4-*cis* (98 %) liquid PI and PB were modified in 3 steps to graft furanic groups that could react with a bis-maleimide compound to yield thermo-reversible elastomeric networks based on the Diels-Alder reaction. The use of liquid polymers as starting materials allowed an easier control of the chemical modifications, the washing steps and the processing compared to highly viscous high molar mass polymer generally used in such studies. The mechanical properties of the networks can be easily tuned by modifying the ratio between the furan and the maleimide moieties. A family of elastomer exposing a wide range of mechanical properties has been obtained. The storage modulus could vary for instance between 1 and 300 MPa in the rubbery plateau whereas the strain at break can be comprised between 1 and 20 MPa. In addition, these elastomers showed a thermal stability up to 110-120 °C. No properties loss has been observed after 5 cycles of reprocessing, showing the good thermal and mechanical resistance of these elastomers.

Experimental

Materials

Cis-1,4-polybutadiene (98 % *cis*-1,4, $M_n = 150 \text{ kg}\cdot\text{mol}^{-1}$, $D = 2.8$) and *cis*-1,4-polyisoprene (98 % *cis*-1,4, $M_n = 635 \text{ kg}\cdot\text{mol}^{-1}$, $D = 2.1$) were purchased from Scientific Polymer Products, Inc. 3-Chloroperoxybenzoic acid (mCPBA, 70-75 %, Acros), periodic acid (H_5IO_6 , $\geq 99 \%$, Aldrich), acetic acid (99 %, Aldrich), sodium bis(2-methoxyethoxy)aluminumhydride (Red-Al[®]) (60 wt. % in

toluene, Aldrich), sodium triacetoxyborohydride ($\text{NaBH}(\text{OAc})_3$, 97 %, Aldrich), diethanolamine (DEA, 99 %, Alfa Aesar), furfuryl isocyanate (Furfuryl-NCO, 97 %, Aldrich), 1,1'-(methylenedi-4,1-phenylene)bismaleimide (Bis-maleimide, 95 %, Alfa Aesar), celite 545 (VWR), dibutyltin dilaurate (DBTDL, 95 %, TCI) were used without further purification. Tetrahydrofuran (THF) and dichloromethane (DCM) were dried on alumina column. Chloroform (CHCl_3), methanol and diethyl ether (reagent grade, Aldrich) were used as received.

CT-PI synthesis

High molar mass *cis*-1,4-polyisoprene (4.28 g), solubilized in 150 mL of THF, was first epoxidized by a dropwise addition at 0 °C of a mCPBA solution (0.805 mmol in 10 mL of THF). After 2h of reaction at room temperature, periodic acid (1.05 eq. compared to mCPBA, 0.846 mmol), dissolved in 10 mL of THF, was added dropwise and stirred during 2h at room temperature. The solvent was then removed under reduced pressure and the crude product was dissolved in diethyl ether before filtration on celite to remove insoluble iodic acid. The filtrate was then concentrated before washing 2 times with saturated solution (30 mL of each) of $\text{Na}_2\text{S}_2\text{O}_3$, NaHCO_3 and distilled water. Finally, the organic layer was dried with MgSO_4 , filtered on celite and the solvent was evaporated under vacuum to obtain CT-PI $M_n(\text{NMR}) = 9\,000 \text{ g}\cdot\text{mol}^{-1}$, $M_n(\text{SEC}) = 11\,400 \text{ g}\cdot\text{mol}^{-1}$, $D = 1.4$. Yield = 94 %. $^1\text{H NMR}$ (400 MHz, CDCl_3): (δ , ppm) 9.77 (t, 1H, $-\text{CH}_2\text{-CHO}$), 5.12 (s, nH, $-\text{CH}_2\text{-C}(\text{CH}_3)=\text{CH-CH}_2-$), 2.49 (t, 2H, $-\text{CH}_2\text{-CHO}$), 2.44 (t, 2H, $-\text{CH}_2\text{-CH}_2\text{-C}=\text{O}(\text{CH}_3)$), 2.34 (t, 2H, $-\text{CH}_2\text{-CH}_2\text{-CHO}$), 2.27 (t, 2H, $-\text{CH}_2\text{-CH}_2\text{-C}=\text{O}(\text{CH}_3)$), 2.12 (s, 3H, $-\text{CH}_2\text{-CH}_2\text{-C}=\text{O}(\text{CH}_3)$), 2.04 (s, 4nH, $-\text{CH}_2\text{-C}(\text{CH}_3)=\text{CH-CH}_2-$), 1.68 (s, 3nH, $-\text{CH}_2\text{-C}(\text{CH}_3)=\text{CH-CH}_2-$) with $n = 130$.

CT-EPI synthesis

CT-PI (4.2 g, 61.76 mmol isoprene units) solubilized in 150 mL of THF was partially epoxidized by a dropwise addition at 0 °C of a mCPBA solution (6.17 mmol in 10 mL of THF, 10 mol%

compared to isoprene units). After 2h of reaction at room temperature, the solution was concentrated before being washed 3 times by precipitation/dissolution in methanol/DCM and the solvent was evaporated under vacuum to obtain CT-EPI. The epoxy percentage was determined by ^1H NMR with the formula $\text{Epoxy (\%)} = [I(2.69) / I(2.69 + 5.12)] \times 100$, Epoxy content = 10.0 %, Yield: 95 %. ^1H NMR (400 MHz, CDCl_3): (δ , ppm) 9.77 (t, 1H, $-\text{CH}_2\text{-CHO}$), 5.12 (s, n-mH, $-\text{CH}_2\text{-C}(\text{CH}_3)=\text{CH-CH}_2-$), 2.68 (t, mH, $-\text{CH-epoxy-CH}_3-$), 2.49 (t, 2H, $-\text{CH}_2\text{-CHO}$), 2.44 (t, 2H, $-\text{CH}_2\text{-CH}_2\text{-C=O}(\text{CH}_3)$), 2.34 (t, 2H, $-\text{CH}_2\text{-CH}_2\text{-CHO}$), 2.27 (t, 2H, $-\text{CH}_2\text{-CH}_2\text{-C=O}(\text{CH}_3)$), 2.04 (s, 4(n-m)H, $-\text{CH}_2\text{-C}(\text{CH}_3)=\text{CH-CH}_2-$), 1.68 (s, 3(n-m)H, $-\text{CH}_2\text{-C}(\text{CH}_3)=\text{CH-CH}_2-$), 1.28 (s, 3mH, $-\text{CH-epoxy-CH}_3-$) with $n = 130$ and $m = 13$.

PI-OH synthesis

CT-EPI (4.20 g, 6.18 mmol oxirane units) solubilized in 84 mL of dry toluene was reduced by addition at room temperature of a Red-Al solution (6 eq compared to oxirane units, 12.5 mL). After stirring at 110 °C during 16h, 30 mL of toluene were added, and the residual Red-Al was deactivated at 0 °C by a dropwise addition of ethanol and water. The solution was then dried with MgSO_4 before filtration onto Celite. The organic solvent was evaporated under vacuum to obtain PI-OH. Yield = 92 %. ^1H NMR (400 MHz, CDCl_3): (δ , ppm) 5.13 (s, n-mH, $-\text{CH}_2\text{-C}(\text{CH}_3)=\text{CH-CH}_2-$), 3.80 (t, 4H, $-\text{CH}_2\text{-OH}$), 3.74 , 3.62 (m, mH, $-\text{CH}(\text{OH})$), 2.04 (s, 4(n-m)H, $-\text{CH}_2\text{-C}(\text{CH}_3)=\text{CH-CH}_2-$), 1.68 (s, 3(n-m)H, $-\text{CH}_2\text{-C}(\text{CH}_3)=\text{CH-CH}_2-$) with $n = 130$ and $m = 13$

PI-Fur synthesis

PI-OH (3.88 g, 5.71 mmol -OH groups) was solubilized in 25 mL of dry THF. 1.2 eq of furfuryl-NCO (732 μL , 6.85 mmol) and 5 mol% of DBTDL (168 μL , 0.28 mmol) were added to the solution and stirred at 40 °C during 6h under inert atmosphere. After partial evaporation of the solvent, the product was purified by precipitation/dissolution in methanol/DCM several times and dried in

vacuum to obtain a brown liquid PI-Fur. Yield = 92 %. $^1\text{H NMR}$ (400 MHz, CDCl_3): (δ , ppm) 7.32 (m, mH, $-\text{CH}=\text{CH}-\text{O}$ - furan), 6.29 (m, mH, $-\text{CH}=\text{CH}-\text{O}$ - furan), 6.18 (m, mH, $\text{C}=\text{CH}-\text{CH}=\text{CH}-\text{O}$ - furan), 5.12 (m, $2(n-m)\text{H}$, $-\text{CH}_2-\text{C}(\text{CH}_3)=\text{CH}-\text{CH}_2-$), 4.34 (s, mH, $-\text{CH}$ (urethane) along the chain), 4.27 (s, $(2m+4)\text{H}$, $-\text{NH}-\text{CH}_2$ -furan), 4.06 (t, 2H, urethane- CH_2-CH_2 - chain-ends), 2.04 (s, $4(n-m)\text{H}$, $-\text{CH}_2-\text{C}(\text{CH}_3)=\text{CH}-\text{CH}_2-$), 1.68 (s, $3(n-m)\text{H}$, $-\text{CH}_2-\text{C}(\text{CH}_3)=\text{CH}-\text{CH}_2-$) with $n = 130$ and $m = 13$.

AT-PB synthesis

High molar mass *cis*-1,4-polybutadiene (3.09 g) solubilized in 110 mL of THF was first epoxidized by a dropwise addition at 0 °C of a mCPBA solution (0.59 mmol in 10 mL of THF). After 2h of reaction at room temperature, periodic acid (1.05 eq. compared to mCPBA, 0.62 mmol) dissolved in 10 mL of THF was added dropwise and stirred during 2h at room temperature. The solvent was then removed under reduced pressure and the crude product was dissolved in diethyl ether before filtration on celite to remove insoluble iodic acid. The filtrate was then concentrated before washing 2 times with saturated solution (30 mL of each) of $\text{Na}_2\text{S}_2\text{O}_3$, NaHCO_3 and distilled water. Finally, the organic layer was dried with MgSO_4 , filtered on celite and the solvent was evaporated under vacuum to obtain AT-PB. $M_n \text{ NMR} = 10\,250 \text{ g}\cdot\text{mol}^{-1}$, $M_n \text{ SEC} = 12\,400 \text{ g}\cdot\text{mol}^{-1}$, $D = 1.7$, yield: 94 %. $^1\text{H NMR}$ (400 MHz, CDCl_3): (δ , ppm) 9.77 (t, 2H, $-\text{CH}_2-\text{CHO}$), 5.38 (m, 2nH, $-\text{CH}_2-\text{CH}=\text{CH}-\text{CH}_2-$), 2.49 (t, 4H, $-\text{CH}_2-\text{CH}_2-\text{CHO}$), 2.38 (t, 4H, $-\text{CH}_2-\text{CH}_2-\text{CHO}$), 2.09 (s, 4nH, $-\text{CH}_2-\text{CH}=\text{CH}-\text{CH}_2-$) with $n = 187$

AT-EPB synthesis

AT-PB (2.83 g, 52.41 mmol butadiene units) solubilized in 100 mL of THF was epoxidized by a dropwise addition at 0 °C of a mCPBA solution (5.76 mmol in 10 mL of THF). After 2h of reaction at room temperature, the solution was concentrated before being washed 3 times by

precipitation/dissolution in methanol/DCM and the solvent was evaporated under vacuum to obtain AT-EPB. The epoxy percentage was determined by ^1H NMR with the formula Epoxy (%) = $[I(2.79) / I(2.79 + 5.24)] \times 100$, Epoxy content = 11.2 %, Yield: 93 %. ^1H NMR (400 MHz, CDCl_3): (δ , ppm) 9.77 (t, 2H, $-\text{CH}_2\text{-CHO}$), 5.38 (m, 2(n-m)H, $-\text{CH}_2\text{-CH=CH-CH}_2-$), 2.92 (t, 2mH, $-\text{CH-epoxy-CH-}$), 2.49 (t, 4H, $-\text{CH}_2\text{-CH}_2\text{-CHO}$), 2.38 (t, 4H, $-\text{CH}_2\text{-CH}_2\text{-CHO}$), 2.22 (m, 2mH, $-\text{CH}_2\text{-CH-epoxy-CH-CH}_2-$), 2.08 (s, 4(n-m)H, $-\text{CH}_2\text{-CH=CH-CH}_2-$) with n = 187 and m = 21

PB-OH synthesis

AT-EPB (2.70 g, 5.00 mmol of oxirane units) solubilized in 30 mL of dry toluene was oxidized by addition at room temperature of a Red-Al solution (6 eq compared to oxirane units, 10.1 mL). After stirring at 110 °C during 16h, 30 mL of toluene were added, and the residual Red-Al was deactivated at 0 °C by a dropwise addition of ethanol and water. The solution was then dried with MgSO_4 before filtration onto Celite. The organic solvent then evaporated under vacuum to obtain PB-OH. Yield = 83 %. ^1H NMR (400 MHz, CDCl_3): (δ , ppm) 5.38 (m, 2(n-m)H, $-\text{CH}_2\text{-CH=CH-CH}_2-$), 3.64 (t, 4H, $-\text{CH}_2\text{-OH}$), 3.60 (m, mH, $-\text{CH(OH)}$), 2.08(s, 4(n-m)H, $-\text{CH}_2\text{-CH=CH-CH}_2-$) with n = 187 and m = 21.

PB-Fur synthesis

PB-OH (2.14 g, 4.36 mmol -OH groups) was solubilized in 14 mL of dry THF. 1.2 eq of furfuryl-NCO (560 μL , 5.23 mmol) and 5 mol% of DBTDL (128 μl , 0.22 mmol) were added to the solution and stirred at 40 °C during 6h under inert atmosphere. After concentration, the product was purified by precipitation/dissolution in methanol/DCM several times and dried under vacuum to obtain a brown liquid PB-Fur. Yield = 92 %. ^1H NMR (400 MHz, CDCl_3): (δ , ppm) 7.34 (m, mH, $-\text{CH=CH-O- furan}$), 6.30 (m, mH, $-\text{CH=CH-O- furan}$), 6.20 (m, mH, $-\text{C=CH-CH=CH-O- furan}$), 5.38 (m, 2(n-m)H, $-\text{CH}_2\text{-CH=CH-CH}_2-$), 4.78 (s, mH, $-\text{CH(urethane)}$ along the chain), 4.33 (s, (2m+4)H, -

NH-CH₂-furan), 4,08 (t, 4H, -CH₂-urethane chain-ends) , 2.08 (s, 4(n-m)H, -CH₂-CH=CH-CH₂-) with n = 187 and m = 21.

Preparation of network films

Networks of PI and PB were obtained by mixing the dissolved PI/PB-Fur in chloroform with the adequate quantity of bis-maleimide dissolved in chloroform. The mixture was heated at 60 °C for 10 min in a closed glassware and deposited in a Teflon mold. Solvent was then let evaporated for 24h and complete drying was obtained under vacuum for an extra 24h to obtain a transparent film without air bubble. For example, the Net-PI-1.00 eq was obtained by mixing 818 mg of PI-Fur in 1 mL of chloroform with 219 mg of bismaleimide in 1 mL of chloroform. (219 = 32 mg + 187 mg corresponding to chain-ends furans, calculated via the DP and to the furan along the chain calculated with the percentage of epoxy content, detailed in ESI).

Swelling tests

Dried samples (initial mass, m_i , approximately 40 mg) were placed into chloroform at room temperature for 24h. Chloroform was changed, and samples were placed again for 48h at room temperature. Swollen samples were weighted (swollen mass, m_s) and dried under vacuum until constant mass (dry mass, m_d). Each sample was analyzed in triplicates. Swelling degree and the soluble fraction were determined by Eqs. 1 and 2 respectively.

$$\text{Swelling degree} = (m_s - m_d) / m_d \times 100 (\%) \quad (\text{equation. 1})$$

$$\text{Soluble fraction} = (m_i - m_d) / m_i \times 100 (\%) \quad (\text{equation. 2})$$

Films remolding

All the strips used for DMA and tensile tests analyses were put into a hermetic closed glassware (1 g in 1.5 mL of CHCl₃, the best solvent to solubilize the prepolymers) and heated at 120 °C for 10 minutes. After 5 minutes at room temperature, the liquid solution is deposited in a Teflon mold

before waiting 24h for solvent evaporation and an extra 24 h under vacuum to obtain a transparent film without air bubble.

Characterization

Liquid-state ^1H and ^{13}C NMR spectra were recorded at 298 K on a Bruker Avance 400 spectrometer operating at 400 MHz and 100 MHz respectively in CDCl_3 . Polymer molar masses were determined by size exclusion chromatography (SEC) using tetrahydrofuran (THF) as the eluent (THF with 250 ppm of Butylated hydroxytoluene as inhibitor, Aldrich) at 40 °C. The SEC line was equipped with a Waters pump, a Waters RI detector and a Wyatt Light Scattering detector. The separation was achieved on three Tosoh TSK gel columns (300×7.8 mm) G5000 HXL, G6000 HXL and a Multipore HXL with exclusion limits from 500 to 40 000 000 g/mol, at flow rate of 1 mL/min. The injected volume is 100 μL . Molar masses were evaluated with polyisoprene standards calibration. Data were processed with Astra software from Wyatt. Differential scanning calorimetry (DSC) measurements of rubber samples (≈ 10 mg) were performed using a DSC Q100 LN_2 apparatus from TA Instruments with a heating and cooling ramp of 10 °C.min $^{-1}$. The samples were first heated from 25 °C to 80 °C and held at 80 °C for 10 min in order to eliminate the residual solvent, then cooled to -150 °C and finally heated to 200 °C. The analyses were carried out in a helium atmosphere with aluminum pans. Thermo-gravimetric measurements (TGA) of polybutadiene samples (≈ 12 mg) were performed on a TA Instruments Q500 from room temperature to 600 °C with a heating rate of 10 °C.min $^{-1}$. The analyses were investigated under nitrogen atmosphere with platinum pans. A TA Instrument RSA3 was used to study dynamic mechanical properties of rubber samples. They were analyzed under air atmosphere from - 105 °C to 200 °C at a heating rate of 4 °C.min $^{-1}$. The measurements were performed in tensile mode at a frequency of 1 Hz and an initial static force of 0.1 N. Tensile tests were performed on a MTS Qtest

25 Elite controller (France) at 22 °C. The initial grip separation was set at 20 mm and the crosshead speed at 50 mm/min. The results were obtained from at least 4 replicates for each sample.

AUTHOR INFORMATION

Corresponding author: *E-mail: peruch@enscbp.fr

NOTES

The authors declare no conflicts of interests.

SUPPORTING INFORMATION

Calculation of bis-maleimide contents, SEC chromatograms, NMR spectra, DSC thermograms, Tensile tests curves, Tables for analysis results

ACKNOWLEDGMENT

Pierre Berto thanks the University of Bordeaux for his PhD fellowship.

REFERENCES

- (1) Denissen, W.; Rivero, G.; Nicolaÿ, R.; Leibler, L.; Winne, J. M.; Du Prez, F. E. Vinylogous Urethane Vitrimers. *Adv. Funct. Mater.* **2015**, *25* (16), 2451–2457.
- (2) Polgar, L. M.; van Duin, M.; Broekhuis, A. A.; Picchioni, F. Use of Diels–Alder Chemistry for Thermoreversible Cross-Linking of Rubbers: The Next Step toward Recycling of Rubber Products? *Macromolecules* **2015**, *48* (19), 7096–7105.
- (3) Trovatti, E.; Lacerda, T. M.; Carvalho, A. J. F.; Gandini, A. Recycling Tires? Reversible Crosslinking of Poly(Butadiene). *Adv. Mater.* **2015**, *27* (13), 2242–2245.
- (4) Folmer, B. J. B.; Sijbesma, R. P.; Versteegen, R. M.; van der Rijt, J. a. J.; Meijer, E. W. Supramolecular Polymer Materials: Chain Extension of Telechelic Polymers Using a Reactive Hydrogen-Bonding Synthone. *Adv. Mater.* **2000**, *12* (12), 874–878.

- (5) Courtois, J.; Baroudi, I.; Nouvel, N.; Degrandi, E.; Pensec, S.; Ducouret, G.; Chanéac, C.; Bouteiller, L.; Creton, C. Supramolecular Soft Adhesive Materials. *Adv. Funct. Mater.* **2010**, *20* (11), 1803–1811.
- (6) Yoshida, S.; Ejima, H.; Yoshie, N. Tough Elastomers with Superior Self-Recoverability Induced by Bioinspired Multiphase Design. *Adv. Funct. Mater.* **2017**, *27* (30), 1701670.
- (7) Zhang, H.; Wang, D.; Liu, W.; Li, P.; Liu, J.; Liu, C.; Zhang, J.; Zhao, N.; Xu, J. Recyclable Polybutadiene Elastomer Based on Dynamic Imine Bond. *J. Polym. Sci. Part A: Polym. Chem.* **2017**, *55* (12), 2011–2018.
- (8) Herbst, F.; Döhler, D.; Michael, P.; Binder, W. H. Self-Healing Polymers via Supramolecular Forces. *Macromol. Rapid Commun.* **2013**, *34* (3), 203–220.
- (9) Tang, Z.; Huang, J.; Guo, B.; Zhang, L.; Liu, F. Bioinspired Engineering of Sacrificial Metal–Ligand Bonds into Elastomers with Supramechanical Performance and Adaptive Recovery. *Macromolecules* **2016**, *49* (5), 1781–1789.
- (10) Van Lijsebetten, F.; Spiesschaert, Y.; Winne, J. M.; Du Prez, F. E. Reprocessing of Covalent Adaptable Polyamide Networks through Internal Catalysis and Ring-Size Effects. *J. Am. Chem. Soc.* **2021**, *143* (38), 15834–15844.
- (11) Cordier, P.; Tournilhac, F.; Soulié-Ziakovic, C.; Leibler, L. Self-Healing and Thermoreversible Rubber from Supramolecular Assembly. *Nature* **2008**, *451* (7181), 977–980.
- (12) Hu, W.; Ren, Z.; Li, J.; Askounis, E.; Xie, Z.; Pei, Q. New Dielectric Elastomers with Variable Moduli. *Adv. Funct. Mater.* **2015**, *25* (30), 4827–4836.
- (13) Jin, K.; Li, L.; Torkelson, J. M. Recyclable Crosslinked Polymer Networks via One-Step Controlled Radical Polymerization. *Adv. Mater.* **2016**, *28* (31), 6746–6750.
- (14) Li, L.; Chen, X.; Jin, K.; Rusayyis, M. B.; Torkelson, J. M. Arresting Elevated-

Temperature Creep and Achieving Full Cross-Link Density Recovery in Reprocessable Polymer Networks and Network Composites via Nitroxide-Mediated Dynamic Chemistry. *Macromolecules* **2021**, *54* (3), 1452–1464.

(15) Rivera, M. R.; Nájera, R. H.; Tapia, J. J. B.; Guerrero, L. R. Structure and Properties of Model Polybutadienes - Effect of Microstructure on the Dynamic Mechanical Properties of Rubber. *Journal of Elastomers & Plastics* **2005**, *37* (3), 267–278.

(16) Kumar, R.; Sayala, K. D.; Cao, Y.; Tsarevsky, N. V. Functionalization of Cis-1,4-Polyisoprene Using Hypervalent Iodine Compounds with Tetrazole Ligands. *Journal of Polymer Science* **2020**, *58* (1), 172–180.

(17) Gandini, A. The Furan/Maleimide Diels–Alder Reaction: A Versatile Click–Unclick Tool in Macromolecular Synthesis. *Progress in Polymer Science* **2013**, *38* (1), 1–29.

(18) Chujo, Y.; Sada, K.; Saegusa, T. Reversible Gelation of Polyoxazoline by Means of Diels–Alder Reaction. *Macromolecules* **1990**, *23* (10), 2636–2641.

(19) Zewert, T. E.; Harrington, M. G. Cross-Linked Poly(N-Acetyleneimine) as an Isoelectric Focusing Matrix. *Electrophoresis* **1999**, *20* (7), 1339–1348.

(20) Laita, H.; Boufi, S.; Gandini, A. The Application of the Diels–Alder Reaction to Polymers Bearing Furan Moieties. 1. Reactions with Maleimides. *European Polymer Journal* **1997**, *33* (8), 1203–1211.

(21) Gheneim, R.; Perez-Berumen, C.; Gandini, A. Diels–Alder Reactions with Novel Polymeric Dienes and Dienophiles: Synthesis of Reversibly Cross-Linked Elastomers. *Macromolecules* **2002**, *35* (19), 7246–7253.

(22) Kuang, X.; Liu, G.; Dong, X.; Wang, D. Enhancement of Mechanical and Self-Healing Performance in Multiwall Carbon Nanotube/Rubber Composites via Diels–Alder Bonding.

Macromolecular Materials and Engineering **2016**, *301* (5), 535–541.

(23) Utrera-Barrios, S.; Verdejo, R.; López-Manchado, M. A.; Santana, M. H. Evolution of Self-Healing Elastomers, from Extrinsic to Combined Intrinsic Mechanisms: A Review. *Mater. Horiz.* **2020**, *7* (11), 2882–2902.

(24) Bai, J.; Li, H.; Shi, Z.; Yin, J. An Eco-Friendly Scheme for the Cross-Linked Polybutadiene Elastomer via Thiol–Ene and Diels–Alder Click Chemistry. *Macromolecules* **2015**, *48* (11), 3539–3546.

(25) Wang, D.; Guo, J.; Zhang, H.; Cheng, B.; Shen, H.; Zhao, N.; Xu, J. Intelligent Rubber with Tailored Properties for Self-Healing and Shape Memory. *J. Mater. Chem. A* **2015**, *3* (24), 12864–12872.

(26) Lotti, L.; Coiai, S.; Ciardelli, F.; Galimberti, M.; Passaglia, E. Thiol-Ene Radical Addition of L-Cysteine Derivatives to Low Molecular Weight Polybutadiene. *Macromolecular Chemistry and Physics* **2009**, *210* (18), 1471–1483.

(27) ten Brummelhuis, N.; Diehl, C.; Schlaad, H. Thiol–Ene Modification of 1,2-Polybutadiene Using UV Light or Sunlight. *Macromolecules* **2008**, *41* (24), 9946–9947.

(28) Korthals, B.; Morant-Miñana, M. C.; Schmid, M.; Mecking, S. Functionalization of Polymer Nanoparticles by Thiol–Ene Addition. *Macromolecules* **2010**, *43* (19), 8071–8078.

(29) Lenko, D.; Schlögl, S.; Temel, A.; Schaller, R.; Holzner, A.; Kern, W. Dual Crosslinking of Carboxylated Nitrile Butadiene Rubber Latex Employing the Thiol-Ene Photoreaction. *J. Appl. Polym. Sci.* **2013**, *129* (5), 2735–2743.

(30) Justynska, J.; Hordyjewicz, Z.; Schlaad, H. Toward a Toolbox of Functional Block Copolymers via Free-Radical Addition of Mercaptans. *Polymer* **2005**, *46* (26), 12057–12064.

(31) Leicht, H.; Huber, S.; Göttker-Schnetmann, I.; Mecking, S. Allylboration as a Versatile

Tool for the in Situ Post-Polymerization Functionalization of 1,4-Cis-Poly(Butadiene). *Polym. Chem.* **2016**, *7* (47), 7195–7198.

(32) Tanasi, P.; Hernández Santana, M.; Carretero-González, J.; Verdejo, R.; López-Manchado, M. A. Thermo-Reversible Crosslinked Natural Rubber: A Diels-Alder Route for Reuse and Self-Healing Properties in Elastomers. *Polymer* **2019**, *175*, 15–24.

(33) Berto, P.; Grelier, S.; Peruch, F. Telechelic Polybutadienes or Polyisoprenes Precursors for Recyclable Elastomeric Networks. *Macromol. Rapid Commun.* **2017**, *38* (22), 1700475.

(34) Berto, P.; Pointet, A.; Le Coz, C.; Grelier, S.; Peruch, F. Recyclable Telechelic Cross-Linked Polybutadiene Based on Reversible Diels–Alder Chemistry. *Macromolecules* **2018**, *51* (3), 651–659.

(35) Berto, P.; Grelier, S.; Peruch, F. Controlled Degradation of Polyisoprene and Polybutadiene: A Comparative Study of Two Methods. *Polymer Degradation and Stability* **2018**, *154*, 295–303.

(36) Zhou, Q.; Jie, S.; Li, B.-G. Facile Synthesis of Novel HTPBs and EHTPBs with High Cis-1,4 Content and Extremely Low Glass Transition Temperature. *Polymer* **2015**, *67*, 208–215.

(37) Saetung, A.; Rungvichaniwat, A.; Campistron, I.; Klinpituksa, P.; Laguerre, A.; Phinyocheep, P.; Pilard, J.-F. Controlled Degradation of Natural Rubber and Modification of the Obtained Telechelic Oligoisoprenes: Preliminary Study of Their Potentiality as Polyurethane Foam Precursors. *J. Appl. Polym. Sci.* **2010**, *117* (3), 1279–1289.

(38) Zhou, Q.; Wang, A.; Dai, L.; Jie, S.; Li, B.-G. Cleavable Polybutadiene Rubber: A Versatile Precursor to Hydroxyl-Terminated or Multi-Hydroxyl Polybutadiene and Polyethylene. *Polymer* **2016**, *107*, 306–315.

(39) Roos, K.; Dolci, E.; Carlotti, S.; Caillol, S. Activated Anionic Ring-Opening

Polymerization for the Synthesis of Reversibly Cross-Linkable Poly(Propylene Oxide) Based on Furan/Maleimide Chemistry. *Polym. Chem.* **2016**, 7 (8), 1612–1622.